Bioorganic Chemistry 92 (2019) 103163

Contents lists available at ScienceDirect

Bioorganic Chemistry

journal homepage: www.elsevier.com/locate/bioorg

Synthesis and biological evaluation of a novel series of curcumin-peptide derivatives as PepT1-mediated transport drugs

Jiyun Zhang, Hongmei Wen*, Fei Shen, Xinzhi Wang, Chenxiao Shan, Chuan Chai, Jian Liu, Wei Li*

School of Pharmacy, Nanjing University of Chinese Medicine, Nanjing 210023, PR China

ARTICLE INFO

Keywords:
CUR-peptide conjugates
Antitumor
PepT1
Caco-2 cells
Celluar uptake

ABSTRACT

Curcumin (CUR) is a natural yellow pigment from turmeric with extensive bioactivities. However its relatively poor solubility limited its absorption and bioavailability. In this study, a novel series of **CUR**-peptide conjugates were designed and synthesized as PepT1-mediated transport drugs and their solubility, cellular uptakes and antitumor activities were evaluated. Ten compounds showed better water solubility than **CUR** due to the dipeptide moiety. Compared with **CUR**, compound **5e** exhibited the slightly better activity and **5d** showed the similar activity with **CUR**. Besides, compounds **5d** and **5e** performed higher cellular uptakes in Caco-2 cell and dose-dependently inhibited by the addition of PepT1 typical substrate glycylsarcosine (Gly-Sar). Compound **5d** and **5e** have improved the absorption of CUR by PepT1-mediated without affected the activity. These new dipeptide conjugates of **CUR** may serve as promising lead compounds for future drug development.

1. Introduction

Curcumin (**CUR**, Fig. 1) is a phenolic compound isolated from the rhizome of *Curcuma longa* L. [1], has a wide range of biological activities chemoprevention [2–7]. **CUR** is currently being tested in clinical trials for treatment of various types of cancers, including liver cancer, colon cancer, multiple myeloma etc [8–11]. **CUR** has three functional groups including one active methylene group and two phenolic groups [12]. However, its relatively poor solubility and instability at physiological condition limited its absorption and bioavailability to a great extent, which restricts the therapeutic usage of **CUR** [13,14].

Over the past decade, the human intestinal oligopeptide transporter 1 (PepT1), has been widely explored as a target for increasing the oral bioavailability of poorly absorbed drugs [15–19]. PepT1 is a promising and valuable target protein, responsible for the uptake of dipeptides and tripeptides. Structural information of substrate identified by PepT1 includes: a strong binding site for an *N*-terminal NH_3^+ group; a hydrogen bond to the carbonyl group of the first peptide bond a hydrophobic pocket, which possesses a strong directional vector as indicated; preference for the stereochemistry shown (usually L); acarboxylate binding site [20]. Several dipeptide-drug conjugate (shown in Fig. 2) were synthesized, such as Gly-Val-Acyclovir (**I**), Val-Trp-Acyclovir (**II**) [21,22], Val-Val-Doxorubicin (**III**) [23], Pro-Ile-Zidovudine (**IV**) [24], Val-Ala-Oleanolic Acid (**V**) [25], Phe-Gly-Zidovudine (**VI**) [26], Gly-Val-Saquinvair (**VII**) [27] and they appeared to combine both chemical stability and good affinity for the PepT1 transporter, the peptide carrier strategy applied to improve oral absorption and bioavailability via targeting the PepT1 transporter. The structure and biochemical characteristics of Caco-2 cells are similar to those of human intestinal epithelial cells, various transporters and metabolic enzymes in intestinal epithelial cells could be expressed in Caco-2 cells. Caco-2 cells were an ideal model for studying absorption and transport of drugs, Caco-2 cell model is currently used by most laboratories to evaluating PepT1 transport activity [28,29].

In recent years, diester of **CUR** with valine, glutamic acid and demethylenated piperic acid have been prepared [30–32], several **CUR** derivatives have better water solubility or greater bioavailability, however few of them exhibited more potent anticancer activity than **CUR**, the reason for decreased activity was the phenolic hydroxyl groups of this derivatives were substituted. It had been found that the C4′ phenolic hydroxyl group of **CUR** has a great influence on the tumor activity, and when it modified to an ether, an ester or other groups, the antitumor activity was enhanced [33–35].

In this work, with the aim to further improve the solubility and oral absorption of **CUR**, the structure of parent drugs selected for PepT1-targeted was designed, the phenolic hydroxyls group of **CUR** was acylated with the dipeptide group of amino to form the ether conjugate through a chloroacetic chloride linker and simultaneously the other

* Corresponding authors.
E-mail addresses: njwenhm@126.com (H. Wen), liwaii@126.com (W. Li).

https://doi.org/10.1016/j.bioorg.2019.103163
Received 8 March 2019; Received in revised form 23 July 2019; Accepted 29 July 2019
Available online 06 August 2019

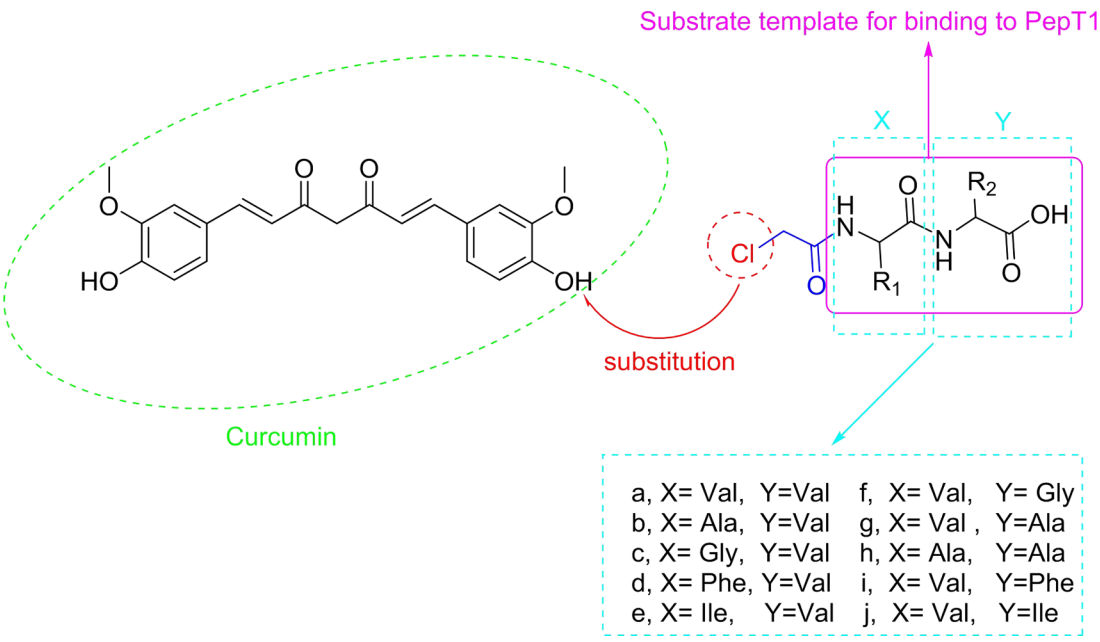

Fig. 1. The structures of novel designed of curcumin-dipeptide derivatives.

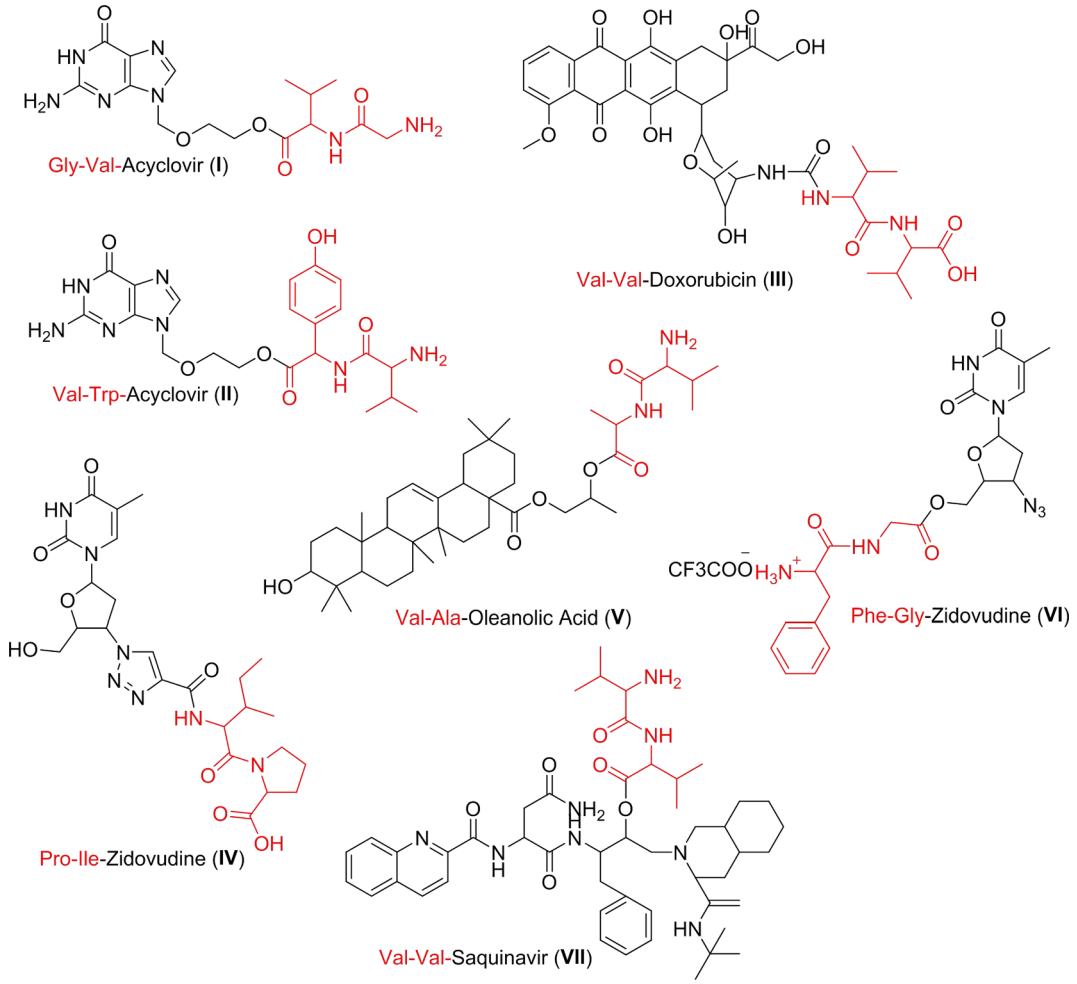

Fig. 2. Dipeptide-drug conjugate as substrates for PepT1.

phenolic hydroxyl group was retained. Ten novel **CUR**-dipeptide bioconjugates **5a-j** were synthesized (Fig. 1) and their solubility, cellular uptakes and anti-tumor activities were evaluated. The equilibrium solubility was assessed by HPLC in ammonia water (pH = 8). The MTT assay was used to evaluate their anti-proliferative activities against HepG2 and SMMC-7721 cells *in vitro*. PepT1-mediated uptake and

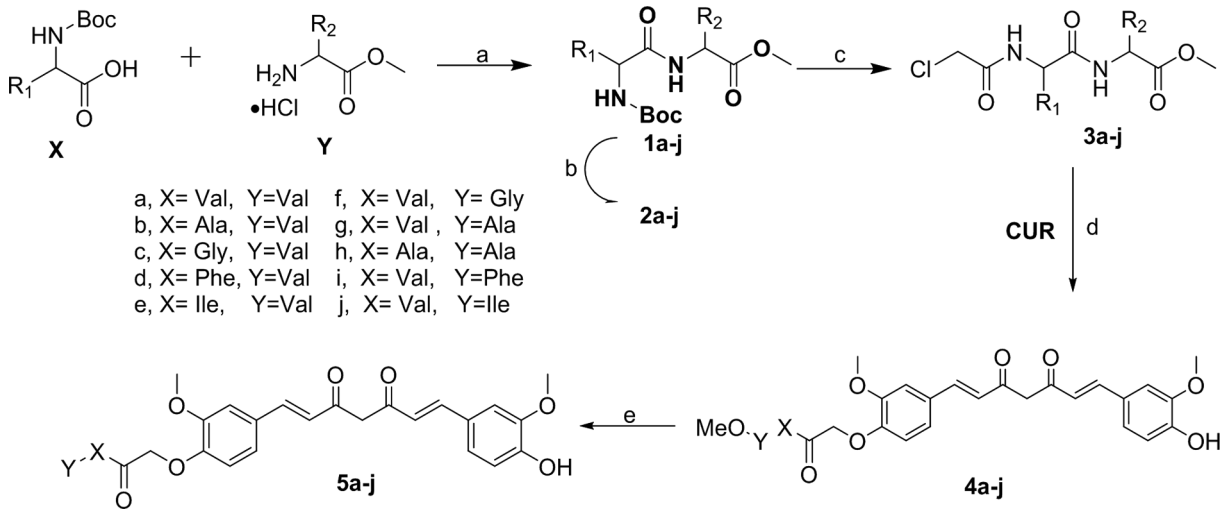

Scheme 1. Synthesis of target compounds **5a-j**. Reagents and condition: (a) DCC, TEA, chloroform, 0 °C 3 h, RT 12 h; (b) TFA, anhydrous CH_2Cl_2; (c) chloroacetyl chloride, TEA, anhydrous CH_2Cl_2; (d) K_2CO_3, KI, acetone; (e) LiOH, MeOH/THF/H_2O.

uptake inhibition studies were determined by LC-MS/MS in Caco-2 cells. *In vitro* phase I metabolism assay was carried out to determined biotransformation of **5d** and **5e**.

2. Results and discussion

2.1. General synthesis procedure for compounds 5a-j

General methods. All reagents involved in the synthesis were used directly without further purification. The preparation of target compounds **5a-j** was described in Scheme 1. The reaction of *N*-Boc-amino acids and amino acid methyl esters was condensed in chloroform in the presence of dehydrating agents *N*,*N*-dicyclohexylcarbodiimide (DCC) and triethylamine (TEA) as catalysts. The *N*-Boc protection of amino group in dipeptides were deprotected with Trifluoroacetate (TFA) (20%) in dry dichloromethane, the reaction time was 1–2 h. Next free amine group is acylated by chloroacetyl chloride in dry dichloromethane. Chlorine was replaced by the phenolic hydroxyl group of **CUR**, then the methyl ester group is removed under alkaline conditions. Compounds **5a-j** were characterized by ^{1}H NMR, ^{13}C NMR and HRMS-ESI.

2.2. Solubility of CUR-dipeptide conjugates

The poor aqueous solubility of **CUR** is the major problem limiting its application. To investigate whether the aqueous solubility of the derivatives was improved, test compounds were selected to determine the equilibrium solubility in ammonia water (pH = 8) according to the Higuchi and Connor's method [36].

The solubility of all compounds were shown in Table 1. It is shown in Table 1 that 10 novel **CUR** derivatives have synthesized and their equilibrium solubility in ammonia water were significantly increased compared with **CUR**. The effects revealed that the conjugation of the phenolic group to dipeptide moiety via an ether linkage improved the water solubility of **CUR**, The phenolic methoxyl groups of **CUR** was linked to dipeptide, solubilities were all enhanced and it as a result of compounds **5a-j** containing carboxylic group. The dipeptide promoiety can improve the hydrophilicity of **CUR**. Reasons for different degrees of water-solubility enhancement of derivatives may be that along with the increase of the carbon number of the substituent, the liposolubility generally increased and the water solubility decreased.

2.3. Antitumor activity of CUR and its derivatives in vitro

To explore the antitumor effect of these compounds, we evaluated their anti-proliferative activities against HepG2 and SMMC-7721 *in vitro* by MTT assay. The half maximal inhibitory concentrations (IC_{50}) of HepG2 and SMMC-7721 cells were described in Table 1 and inhibition of tested compounds on HepG2 cell and SMMC-7721 was shown in Table S1, S2 (shown in Supplementary material). Cell viability rate of compounds **CUR**, **5d** and **5e** *in vitro* antitumor activity of SMMC-7721 and HepG2 was shown in Fig. 3.

As indicated in Table 1, Table S1, S2, **CUR**-dipeptide conjugates have different degrees of inhibition of cell proliferation on HepG2 and SMMC-7721 cells. Several of the **CUR**-dipeptide products exhibited increased antitumor activity toward HepG2 and SMMC-7721 cells compared to that of the parent molecule (**CUR**), while others showed decreased activity. It could be found in Fig. 3 that **CUR**, **5d** and **5e** have obvious antitumor activities. The IC_{50} values of **CUR**, **5d** and **5e** against HepG2 cells were 35.8 μM, 40.2 μM and 23.4 μM; the IC_{50} values of **CUR**, **5d** and **5e** against SMMC-7721 cells were 22.9 μM, 35.4 μM and 19.7 μM. It is also evident from Table 1 that **5e** exhibited increased cellular inhibition toward HepG2 and SMMC-7721 compared to that of

Table 1
Structures, solubility and IC_{50} values of **CUR** and its derivatives **5a-j** against HepG2 and SMMC-7721 cells.

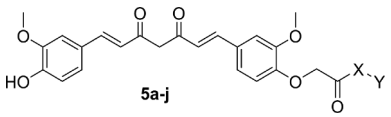

Compounds	X=	Y=	Solubility (mg/ml)	IC50 (μM)	
				HepG2	SMMC-7721
CUR			0.01 ± 0.00	35.8	22.9
5a	Val	Val	3.24 ± 1.32	77.9	82.3
5b	Ala	Val	1.24 ± 0.35	> 100	> 100
5c	Gly	Val	4.52 ± 0.37	92.5	68.8
5d	Phe	Val	1.05 ± 0.14	40.2	35.4
5e	Ile	Val	3.52 ± 0.48	23.4	19.7
5f	Val	Gly	2.22 ± 1.29	80.1	89.3
5g	Val	Ala	1.26 ± 0.74	81.0	90.5
5h	Ala	Ala	2.65 ± 0.32	> 100	> 100
5i	Val	Phe	1.31 ± 0.71	77.3	80.7
5j	Val	Ile	3.72 ± 1.59	71.4	48.6

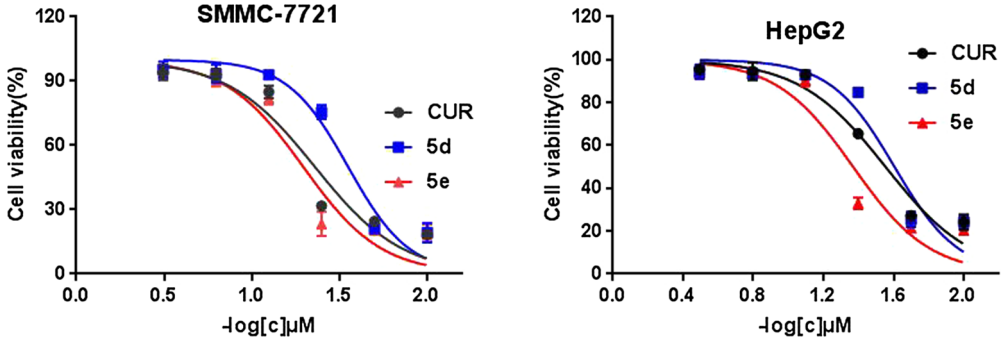

Fig. 3. Cell viability rate of *in vitro* antitumor activity of human hepatoma cell line SMMC-7721 and HepG2.

the **CUR**, **5d** performed almost the resemble activity as the parent drug. Besides, when X was Ala, anti-tumor activities of **5b** and **5h** almost disappeared. While the benzyl substituent (**5d**) was replaced with 2-methyl butyl group (**5e**), the activity was becoming decreased. The **5c** demonstrated the best solubility, however it has relatively weak activity, which showed that great anti-tumor activity requires appropriate liposolubility. The antitumor activity of **5d** (X = Phe, Y = Val) was better than that of **5i** (X = Val, Y = Phe), which explained that X = Phe plays a great important role in anti-tumor activity. This observation encouraged us to prepare the **CUR** derivatives modifying with rational substituents to improve its solubility and inhibition on human hepatoma cell line.

2.4. Uptake and PepT1-mediated inhibition studies

Compound**s** were carried out uptake studies using caco-2 cell and LC-MS/MS method. The inhibition study was evaluated whether PepT1 was involved in **5d** and **5e** cellular uptake. The LC-MS/MS method was established to determine the cellular uptake of **CUR**, **5d** and **5e**. Moreover, the conditions of chromatography and mass spectrometry were optimized, selectivity and linear range were investigated (shown in Table S3). Effects of pH, uptake time, concentration on uptake were explored in Caco-2 cells (shown in Fig. 4). The uptake inhibition studies was displayed in Fig. 5.

PepT1 employs a proton gradient as the driving force, and its activity is pH dependent. Therefore, two drug solutions with different pH (6.0 and 7.4) were used in the uptake studies. From Fig. 4A, cellular uptake was significantly enhanced in pH 6.0 compared to that in pH 7.4, respectively. pH 6.0 was selected in the subsequent experiments. The time-dependent curves (Fig. 4A) indicated that as the uptake time increased, the uptake of the drug in Caco-2 cells also increased, and the uptake rate was faster at 60 min, thus the appropriate uptake time was selected 60 min in the subsequent experiments. The cellular uptakes of **CUR**, **5d** and **5e** were increased in a dose-dependent manner (Fig. 4B), however, compared to **CUR**, compounds **5d** and **5e** all showed obvious higher cellular uptakes at the same concentration, especially at 100 μM. These findings suggested that PepT1 might be involved in the uptake of **5d** and **5e**. To prove the assumption that the increase in the uptake of the **5d** and **5e** was possibly due to the recognition of the **5d** and **5e** by the PepT1, the uptake inhibition test with Gly-Sar (a specific of PepT1 substrate transporters) was performed. The Caco-2 monolayers were incubated with **CUR**, **5d** and **5e** (100 μM) in the absence or in the presence of Gly-sar. As shown in Fig. 5A, there was no difference in the uptake of **CUR** with or without the presence of Gly-Sar, reflecting its poor affinity for the PepT1 transporter in Caco-2 cells, but **5d** and **5e** were significantly reduced at in the presence of Gly-sar, indicating that **5d** and **5e** have an affinity for the PepT1 transporter. To further evaluate the affinity of the **5d** and **5e** to PepT1, **5d** and **5e** were incubated with Gly-Sar at various concentrations (100, 200, 400, 800 μM) in Caco-2 cells. The uptakes of both **5d** (IC_{50} = 148.5 μM) and **5e** (IC_{50} = 145.6 μM) by Caco-2 cells were significantly and dose-dependently inhibited by the addition of PepT1 substrate for 60 min (shown in Fig. 5B). These results demonstrated that **5d** and **5e** have high affinity to PepT1. The dipeptide structure of promoiety **5d** and **5e** may be recognized by the PepT1 and PepT1 might be involved in the uptake of **5d** and **5e**.

2.5. In vitro phase I metabolism assay

To investigate the metabolites of **5d** and **5e**, **5d** and **5e** were incubated with rat liver microsomes determined by LC-QTOF MS method. The high resolution MS/MS fragment ions were listed in Table 2, MS/MS spectra was shown in Figs. S22–30. The mass spectra of **M1** and **M4** showed an $[M-H]^-$ ion at *m/z* 367.1191 ($C_{21}H_{20}O_6$), as shown in Table 2 and Figs. S22, S24, S28, the MS/MS fragment ions of **M1** and **M4** resembled that of **CUR**. Consequently, **M1** and **M4** were assigned as **CUR**, it was suggested that **5d** and **5e** could be metabolized into **CUR**, **5d** and **5e** were the prodrug of **CUR**. Besides the tetrahydro reduction

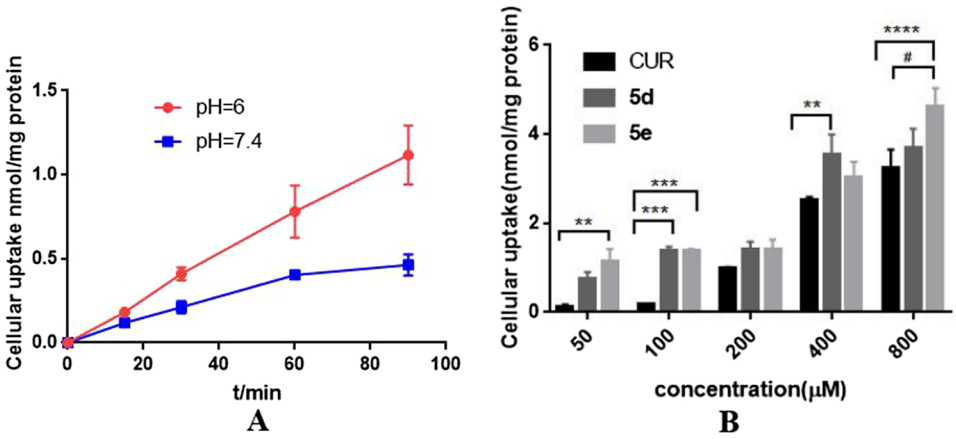

Fig. 4. Uptake studies in Caco-2. (A) Effect of pH and time on cellular uptake of **5d** in Caco-2 cells. Cellular uptake was measured in confluent of Caco-2 at 0, 15, 30, 60, 90 min at pH6.0 or pH7.4. (B) Concentration dependence of **CUR**, compounds **5d** and **5e** uptake in Caco-2 cells with incubated at 37 °C for 60 min with various concentrations at pH 6.0. Statistical differences of each point were compared with CUR groups by a Two-way ANOVA with $p < 0.05$ as the limit of significance (**P < 0.01, ***P < 0.001, ****P < 0.0001); #P < 0.05, compared with compound **5d**, data are expressed as mean ± SD, n = 3.

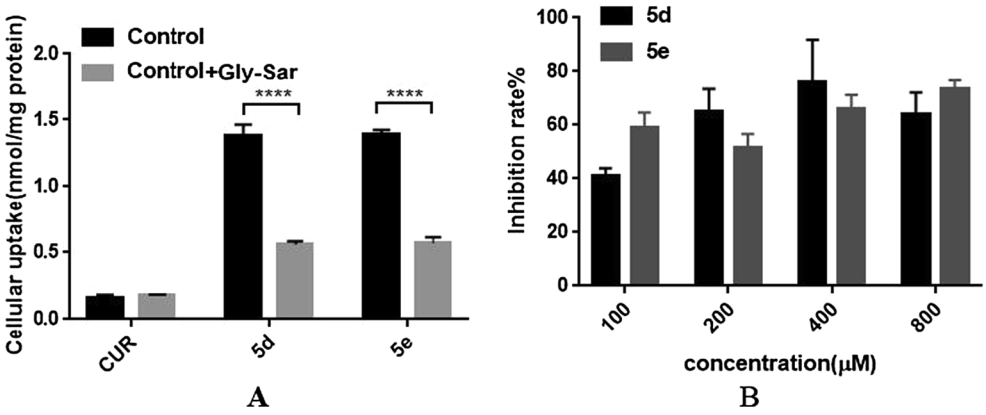

Fig. 5. Uptake PepT1-mediated inhibition studies. (A) The uptake of compounds **CUR**, **5d** and **5e** (100 μM) in the Caco-2 cells with or without the presence of Gly-Sar. (B) The inhibition rate of gly-sar on compounds **5d** and **5e** uptake in the Caco-2 cells. Statistical differences of each point were compared with CUR groups by a Two-way ANOVA with $p < 0.05$ as the limit of significance (**P < 0.01, ***P < 0.001, ****P < 0.0001), data are expressed as mean ± SD, n = 3.

products and hexahydro reduction product of **5d** and **5e** were detected in liver microsome samples.

3. Conclusions

In this study, a novel series of **CUR**-peptide conjugates were designed and synthesized as PepT1-mediated transport drugs and their solubility, cellular uptakes and anti-tumor activities were evaluated. The efficient and easy synthetic procedure has been outlined for the synthesis of ten novel dipeptide conjugates of **CUR**. All of the compounds showed higher water solubility than CUR due to the conjugation of the phenolic group to dipeptide moiety via an ether linkage. These synthesized compounds were evaluated for anti-HepG2 and anti-SMMC-7721 activity by MTT assay. Compared with **CUR**, compound **5e** exhibited slightly stronger inhibitory activities against two liver cells and compound **5d** showed the similar activity. Besides, compound **5d** and **5e** showed obvious higher cellular uptakes than **CUR** in Caco-2 cell model. The cellular uptakes of **5d** and **5e** were dose-dependently inhibited by PepT1 typical substrate Gly-Sar and attributed to PepT1-mediated uptake. Furthermore metabolites of compound **5d** and **5e** were detected and found CUR in rat liver microsomes by LC-QTOF MS. Overall, these results suggested that compound **5d** and **5e** have improved the absorption of CUR by PepT1-mediated without affected the activity. These new dipeptide conjugates of **CUR** may serve as promising lead compounds for future drug development.

4. Experimental

4.1. Materials and methods

The reagents used in the synthesis process are all purchased from Shanghai Macklin Biochemical Co., Ltd. All reactions were monitored by thin-layer chromatography (TLC) on GF-254 silica gel plates (Tsingdao Silica Gel Corp., Tsingdao, China). A silica gel column was used for flash column chromatography (200–300 mesh, Tsingdao Silica Gel Corp., Tsingdao, China). Visualisation was achieved using UV light (254 nm). ^{1}H and ^{13}C NMR spectra were recorded with a Bruker NMR spectrometer (^{1}H NMR: 500 MHz, ^{13}C NMR: 125 MHz) (Bruker Co., Germany). The deuterated solvent used was DMSO with tetramethylsilane (TMS) as the internal standard. High-resolution electrospray ionization mass spectrometry (HRMS-ESI) was measured using a Triple™ TOF 5600 system (AB SCIEX CO., Foster City, CA) tested in negative ionization mode.

4.2. Synthesis of CUR-dipeptides conjugates

4.2.1. Synthesis of dipeptides (*1a-j*)

Boc-amino acids and amino acid methyl esters were prepared according to literature procedure [37]. Boc-amino acids (10 mmol) was dissolved in chloroform (20 mL) and cooled to 0 °C. To this, *N,N′*-dicyclohexyl carbodiimide (DCC) (2.25 g, 11 mmol) was added with stirring, the amino acid methyl ester hydrochloride (10 mmol) was added followed by Triethylamine (TEA, 10 mmol). Stirring was continued at this temperature for 3 h, then at room temperature for 12 h. The completion of the reaction was assessed by precipitation of dicyclohexylurea (DCU). DCU was filtered off and the filtrate was washed with 1 M HCl (3 × 20 mL), 0.5 M Na_2CO_3 (3 × 20 mL) and water (2 × 10 mL). The organic layer thus collected was dried over anhydrous sodium sulphate and evaporated in vacuum. The residue was dissolved in acetonitrile (20 mL), the undissolved dicyclohexylurea (DCU) present in the solution was filtered. The filterate was evaporated in *vacuum*, which yielded a solid mass.

4.2.2. General method for deprotection of dipeptides (*2a-j*)

1a-j (1 mmol) were dissolved in 4 mL anhydrous dichlormethane at 0 °C. TFA (1 mL) was added dropwise to the stirring solution. After this

Table 2
Analysis of *in vitro* metabolites of CUR, 5d and 5e.

Compounds	Metabolite	Molecular formula	Molecular weight	MS/MS fragment ions
CUR	**CUR**	$C_{21}H_{20}O_6$	368.1260	367.1191, 217.0502, 158.0366, 149.0601, 134.0368
5d	**5d**	$C_{37}H_{40}N_2O_{10}$	672.2683	671.2642, 521.1941, 367.1187, 217.0499, 173.0601
	M1 (**CUR**)	$C_{21}H_{20}O_6$	368.1260	217.0504, 158.0361, 149.0604, 134.0366
	M2 (4H)	$C_{37}H_{44}N_2O_{10}$	676.2996	675.2945, 657.2835, 481.198, 353.1387, 177.0547, 162.0312
	M3 (6H)	$C_{37}H_{46}N_2O_{10}$	678.3152	677.3113, 659.3011, 483.2145, 355.1541, 193.0858, 179.0858
5e	**5e**	$C_{34}H_{42}N_2O_{10}$	638.2840	637.2782, 487.2092, 367.1173, 217.0496, 173.0601
	M4 (**CUR**)	$C_{21}H_{20}O_6$	368.1260	321.2275, 175.0366, 173.0604, 134.0356
	M5 (4H)	$C_{34}H_{46}N_2O_{10}$	642.3152	641.2743, 623.2623, 421.1983, 219.0660, 151.0396
	M6 (6H)	$C_{34}H_{48}N_2O_{10}$	644.3309	643.3254, 625.3146, 449.229, 355.1566, 179.0708, 116.0711

4H-Tetrahydro reduction products.
6H- Hexahydro reduction product.

time, the mixture was allowed to warm to room temperature and stirred for 3.5 h. The solvent was removed under reduced pressure to a small volume, the crude product was not purified and used in next step reaction.

4.2.3. N-Chloroacetyl-Dipeptides (3a-j)

The TEA was added dropwise with stirring to a solution of compounds **2a-j** (l mmol) in anhydrous dichloromethane at 0 °C until pH = 7, which was observed by extensive pH indicator paper. Chloroacetyl chloride (1 mmol) in 2 mL of anhydrous dichloromethane was introduced dropwise to the reaction vessel, and with stirring at 0 °C. Next, the addition is completed, the reaction was stirred 4 h at room temperature. The reaction mixture was washed with water three times. The organic layer was dried over anhydrous sodium sulfate, filtered and concentrated. After removing the solvent by reduced pressure distillation, the solid is obtained finally.

4.2.4. Amino acid derivatives of CUR (4a-j)

To the solution of **CUR** (1 mmol) in acetone (6 mL), and stirred for a few minutes to get a clear solution, Further, potassium carbonate (1.2 mmol) was added, the whole solution stirred for 15 min. Then a solution of compound **3a-j** (1 mmol) in acetone (12 mL) was added, and the mixture was stirred for 10 h. After completion of reaction, reaction mixture was filtered and concentrated in vacuum. The residue was diluted with ethyl acetate and followed by washing with water and brine (100 mL). The organic layer thus collected was dried over anhydrous sodium sulphate and evaporated to dryness under *vacuum* to give a crude product, which was purified by silica gel column chromatography using mixture of ethyl acetate and petroleum ether as eluent.

4.2.5. Deprotection of amino acid derivatives of CUR (5a-j)

4a-j (1 mmol) was dissoved in methanol (MeOH), tetrahydrofuran (THF), H_2O (v/v/v = 1:3:1, 10 mL), lithium hydroxide (LiOH, 4 mmol) was added subsequently, The mixture was stirred at room temperature until the completion of the reaction (2–4 h), as indicated by TLC, where the disappearance of **4a-j** was observed. The reaction mixture evaporated to a small volume, which removed the MeOH and THF, then carefully acidified (1 M HCl aq) to pH 3. Yellow solids precipitated from the aqueous solution, thereafter the precipitate was collected by filtration and washed with water to give the final product **5a-j**.

4.3. Characterization result of 10 target compounds

^{1}H NMR (Figs. S1–S10) and ^{13}C NMR (Figs. S11–S20) spectra of all the final compounds were shown in Supplementary material.

4.3.1. CUR-Val-Val (5a)

^{1}H NMR (500 MHz, DMSO-d_6) δ: 12.57 (s, 1H), 9.70 (s, 1H), 8.17 (d, J = 8.5 Hz, 1H), 7.87 (d, J = 8.5 Hz, 1H), 7.57 (d, J = 15.7 Hz, 2H), 7.40 (s, 1H), 7.34 (s, 1H), 7.24 (d, J = 8.3 Hz, 1H), 7.17 (d, J = 8.3 Hz, 1H), 6.97 (m, 1H), 6.85 (m, 2H), 6.78 (d, J = 15.7 Hz, 1H), 6.09 (s, 1H), 4.65 (s, 2H), 4.43 (m, 1H), 4.11 (m, 1H), 3.87(s, 3H), 3.84 (s, 3H), 2.09–1.97 (m, 2H), 0.92–0.84 (m, 9H), 0.81 (m, 3H); ^{13}C NMR (125 MHz, DMSO-d_6) δ: 183.91, 182.40, 172.66, 170.80, 167.14, 149.42, 149.29, 149.18, 147.97, 141.02, 139.79, 128.77, 126.26, 123.16, 122.60, 122.38, 121.10, 115.69, 114.00, 111.43, 111.06, 100.93, 67.74, 57.31, 56.49, 55.81, 55.69, 31.11, 29.55, 19.06, 19.01, 18.04, 17.62; HRMS-ESI calcd for $C_{33}H_{40}N_2O_{10}$ $[M-H]^-$ 623.2610, found 623.2611.

4.3.2. CUR-Ala-Val (5b)

^{1}H NMR (500 MHz, DMSO-d_6) δ: 9.72 (s, 1H), 8.12 (d, J = 8 Hz,1H), 8.08 (d, J = 8 Hz, 1H), 7.57 (d, J = 15.8 Hz, 2H), 7.39 (s, 1H), 7.33 (s, 1H), 7.23 (d, J = 8.2 Hz, 1H), 7.16 (d, J = 8.2 Hz, 1H), 6.97 (m, 1H), 6.84 (m, 2H), 6.77 (d, J = 15.8 Hz, 1H), 6.09 (s, 1H), 4.60 (s, 2H), 4.52 (m, 1H), 4.16 (m, 1H), 3.87(s, 3H), 3.84 (s, 3H), 2.06 (m, 1H), 1.26 (m,3H), 0.88 (m, 6H); ^{13}C NMR (125 MHz, DMSO-d_6) δ: 184.39, 182.90, 173.27, 172.57, 167.40, 149.87, 149.72, 149.67, 148.44, 141.53, 140.33, 129.18, 126.74, 123.67, 123.02, 122.93, 121.55, 116.16, 114.41, 111.80, 111.39, 101.52, 68.15, 57.63, 56.20, 56.13, 48.05, 30.27, 19.55, 19.16, 18.39; HRMS-ESI calcd for $C_{31}H_{36}N_2O_{10}$ $[M-H]^-$ 595.2297, found 595.2286.

4.3.3. CUR-Gly-Val (5c)

^{1}H NMR (500 MHz, DMSO-d_6) δ: 9.71 (s, 1H), 8.12 (m, 2H), 7.58 (d, J = 15.8 Hz, 2H), 7.39 (s, 1H), 7.33 (s, 1H), 7.24 (d, J = 8.2 Hz, 1H), 7.17 (d, J = 8.2 Hz, 1H), 6.99 (m, 1H), 6.85 (m, 2H), 6.78 (d, J = 15.8 Hz, 1H), 6.09 (s, 1H), 4.61 (s, 2H), 4.28–4.13 (m, 1H), 4.39–4.10 (m, 1H), 3.92–3.88 (m, 2H), 3.87(s, 3H), 3.84 (s, 3H), 2.05 (m, 1H), 0.94–0.80 (m, 6H); ^{13}C NMR (125 MHz, DMSO-d_6) δ: 184.38, 182.91, 173.33, 169.04, 168.17, 149.88, 149.74, 149.66, 148.44, 141.52, 140.34, 129.18, 126.74, 123.67, 123.01, 122.92, 121.55, 116.16, 114.34, 111.80, 111.42, 101.51, 68.20, 57.61, 56.19, 56.13, 41.92, 30.41, 19.56, 18.38; HRMS-ESI calcd for $C_{30}H_{34}N_2O_{10}$ $[M-H]^-$ 581.2142, found 581.2133.

4.3.4. CUR-Phe-Val (5d)

^{1}H NMR (500 MHz, DMSO-d_6) δ: 12.74 (s, 1H), 9.71 (s,1H), 8.29 (d, J = 8.4 Hz, 1H), 8.07 (d, J = 8.4 Hz, 1H), 7.58 (d, J = 15.5 Hz, 2H), 7.36 (d, J = 15.5 Hz, 2H), 7.23 (s, 5H), 7.16 (m, 2H), 6.86 (m, 2H), 6.76 (m, 2H), 6.11 (s, 1H), 4.79 (m, 1H), 4.52 (s, 2H), 4.20 (m, 2H), 3.84 (s, 3H), 3.82 (s, 3H), 3.07 (m, 1H), 2.85 (m, 1H), 2.09 (m, 1H), 0.91 (m, 6H); ^{13}C NMR (125 MHz, DMSO-d_6) δ: 184.37, 182.95, 173.29, 171.42, 167.58, 149.89, 149.80, 149.66, 148.45, 141.52, 141.16, 140.37, 137.73, 129.76, 129.08, 128.47, 126.79, 126.74, 123.68, 123.58, 122.98, 122.93, 121.57, 116.17, 114.19, 111.82, 111.34, 101.51, 67.98, 57.70, 56.16, 56.14, 53.46, 38.27, 30.35, 19.57, 18.48; HRMS-ESI calcd for $C_{37}H_{40}N_2O_{10}$ $[M-H]^-$ 671.2610, found 671.2611.

4.3.5. CUR-Ile-Val (5e)

^{1}H NMR (500 MHz, DMSO-d_6) δ: 8.13 (d, J = 8.5 Hz, 1H), 7.88 (d, J = 8.5 Hz, 1H), 7.57 (d, J = 15.7 Hz, 2H), 7.39 (s, 1H), 7.33 (s, 1H), 7.23 (d, J = 8.3 Hz, 1H), 7.16 (m, 1H), 6.96 (d, J = 8.3 Hz, 1H), 6.85 (m, 2H), 6.80–6.74 (m, 1H), 6.09 (s, 1H), 4.64 (s, 2H), 4.46–4.40 (m, 1H), 4.12 (m, 1H), 3.87(s, 3H), 3.84 (s, 3H), 2.13–2.00 (m, 1H), 1.82–1.71 (m, 1H), 1.46–1.39 (m, 1H), 1.08–0.98 (m, 1H), 0.91–0.77 (m, 12H); ^{13}C NMR (125 MHz, DMSO-d_6) δ: 184.40, 182.88, 173.35, 171.39, 167.58, 149.92, 149.75, 149.63, 148.46, 141.52, 140.30, 129.24, 126.74, 123.66, 123.57, 122.88, 121.59, 116.18, 114.39, 111.82, 111.41, 101.53, 68.16, 57.92, 56.48, 56.25, 56.14, 37.75, 30.15, 24.50, 19.56, 18.57, 15.71, 11.4; HRMS-ESI calcd for $C_{34}H_{42}N_2O_{10}$ $[M-H]^-$ 637.2767, found 637.2761.

4.3.6. CUR-Val-Gly (5f)

^{1}H NMR (500 MHz, DMSO-d_6) δ: 12.61 (s, 1H), 9.69 (s, 1H), 8.46 (d, J = 8.5 Hz,1H), 7.89 (d, J = 8.5 Hz, 1H), 7.57 (d, J = 15.8 Hz, 2H), 7.39 (s, 1H), 7.25 (s, 1H), 7.17 (d, J = 8.2 Hz, 1H), 6.99 (d, J = 8.2 Hz, 1H), 6.92–6.82 (m, 2H), 6.77 (d, J = 15.8 Hz, 1H), 6.09 (s, 1H), 4.65 (s, 2H), 4.31 (m, 1H), 3.87(s, 3H), 3.84 (s, 3H), 3.80 (d, J = 5.8 Hz, 1H), 3.77 (d, J = 5.8 Hz, 1H), 2.03 (m, 1H), 0.86 (m, 6H); ^{13}C NMR (125 MHz, DMSO-d_6) δ: 184.40, 182.90, 171.51, 171.35, 167.75, 149.89, 149.73, 149.69, 148.45, 141.53, 140.32, 129.19, 126.74, 123.67, 123.05, 122.91, 121.57, 116.17, 114.36, 111.85, 111.46, 101.49, 68.11, 57.28, 56.27, 56.15, 41.03, 31.41, 19.56, 18.08; HRMS-ESI calcd for $C_{30}H_{34}N_2O_{10}$ $[M-H]$-581.2142, found 581.2140.

4.3.7. CUR-Val-Ala (5g)

^{1}H NMR (500 MHz, DMSO-d_6) δ: 8.40 (d, J = 8.6 Hz, 1H), 7.85 (d, J = 8.6 Hz, 1H), 7.60 (d, J = 15.8 Hz, 2H), 7.42 (s, 1H), 7.35 (s, 1H), 7.27 (d, J = 8.0 Hz, 1H), 7.19 (d, J = 8.0 Hz, 1H), 7.02 (m, 1H), 6.91–6.84 (m, 2H), 6.79 (d, J = 15.8 Hz, 1H), 6.12 (s, 1H), 4.67 (s, 2H), 4.39–4.33 (m, 1H), 4.23 (m, 1H), 3.90 (s, 3H), 3.87 (s, 3H), 2.03 (m,

1H), 1.31 (m, 3H), 0.88 (m, 6H); ^{13}C NMR (125 MHz, DMSO-d_6) δ: 184.40, 182.88, 174.35, 170.66, 167.64, 149.92, 149.81, 149.68, 148.48, 141.51, 140.27, 129.29, 126.76, 123.64, 123.12, 122.86, 121.61, 116.20, 114.54, 111.93, 111.58, 101.44, 68.25, 57.01, 56.31, 56.19, 47.99, 31.64, 19.50, 18.13, 17.46; HRMS-ESI calcd for $C_{31}H_{36}N_2O_{10}$ $[M-H]^-$ 595.2297, found 595.2283.

4.3.8. CUR-Ala-Ala (**5h**)

^{1}H NMR (500 MHz, DMSO-d_6) δ: 8.29 (d, J = 7.5 Hz, 1H), 8.06 (d, J = 7.5 Hz, 1H), 7.60 (d, J = 15.8 Hz, 2H), 7.41 (s, 1H), 7.35 (s, 1H), 7.27 (d, J = 8.1 Hz, 1H), 7.18 (d, J = 8.1 Hz, 1H), 7.01 (m, 1H), 6.89–6.84 (m, 2H), 6.79 (d, J = 15.8 Hz,1H), 6.12 (s,1H), 4.62 (s, 2H), 4.45 (m, 1H), 4.25 (m, 1H), 3.90 (s, 3H), 3.87 (s, 3H), 1.30 (m, 6H); ^{13}C NMR (125 MHz, DMSO-d_6) δ: 184.37, 182.88, 174.39, 171.93, 167.35, 149.93, 149.80, 149.73, 148.48, 141.48, 140.27, 129.26, 126.76, 123.63, 123.11, 122.88, 121.61, 116.21, 114.57, 111.94, 111.57, 101.44, 68.27, 56.27, 56.19, 48.02, 47.98, 19.13, 17.63; HRMS-ESI calcd for $C_{29}H_{32}N_2O_{10}$ $[M-H]^-$ 567.1984, found 567.1980.

4.3.9. CUR-Val-Phe (**5i**)

^{1}H NMR (500 MHz, DMSO-d_6) δ: 8.36 (d, J = 8.4 Hz, 1H), 7.80 (d, J = 8.4 Hz, 1H), 7.57 (d, J = 15.8 Hz, 2H), 7.40 (s, 1H), 7.33 (s, 1H), 7.28–7.21 (m, 5H), 7.20–7.15 (m, 2H), 6.97 (m,1H), 6.85 (m, 2H), 6.78 (d, J = 15.8 Hz, 1H), 6.09 (s,1H), 4.63 (s, 2H), 4.44 (m, 1H), 4.30 (m, 1H), 3.86 (s, 3H), 3.84 (s, 3H), 3.08 (dd, J = 13.9, 5.1 Hz, 1H), 2.90 (dd, J = 13.9, 5.1 Hz, 1H), 2.05–1.94 (m, 1H), 0.80 (m,6H); ^{13}C NMR (125 MHz, DMSO-d_6) δ: 184.40, 182.87, 173.34, 170.88, 167.58, 149.93, 149.75, 149.64, 148.46, 141.57, 141.53, 140.29, 138.09, 129.53, 129.24, 128.57, 126.80, 126.73, 123.67, 123.09, 122.92, 122.88, 121.57, 116.18, 114.42, 111.84, 111.48, 101.51, 68.15, 57.11, 56.27, 56.15, 54.05, 37.13, 31.53, 19.60, 18.02; HRMS-ESI calcd for $C_{37}H_{40}N_2O_{10}$ $[M-H]^-$ 671.2610, found 671.2610.

4.3.10. CUR-Val-Ile (**5j**)

^{1}H NMR (500 MHz, DMSO-d_6) δ 8.16 (d, J = 8.4 Hz, 1H), 7.87 (d, J = 8.4 Hz, 1H), 7.57 (d, J = 15.8 Hz, 2H), 7.40 (s, 1H), 7.33 (s, 1H), 7.24 (d, J = 8.3 Hz, 1H), 7.16 (d, J = 8.2 Hz, 1H), 6.98 (d, J = 8.4 Hz, 1H), 6.86 (m, 1H), 6.77 (d, J = 15.8 Hz, 2H), 6.09 (s, 1H), 4.65 (s, 2H), 4.42 (m, 1H), 4.16 (m, 1H), 3.87 (s, 3H), 3.84 (s, 3H), 2.05–1.97 (m, 1H), 1.78 (m, 1H), 1.47–1.37 (m, 1H), 1.25–1.15 (m, 1H), 0.85 (m, 12H); ^{13}C NMR (125 MHz, DMSO-d_6) δ: 184.39, 182.88, 173.25, 171.15, 167.63, 149.91, 149.74, 149.64, 148.45, 141.52, 140.29, 129.22, 126.73, 123.66, 123.06, 122.88, 121.57, 116.17, 114.38, 111.84, 111.46, 101.50, 68.15, 56.99, 56.96, 56.26, 56.15, 36.62, 31.64, 25.22, 19.56, 18.14, 15.99, 11.77; HRMS-ESI calcd for $C_{34}H_{42}N_2O_{10}$ $[M-H]^-$ 637.2767, found 637.2767.

4.4. Solubility of CUR-dipeptide conjugates

4.4.1. UPLC (Acquity UPLC, Waters Co., USA) condition

Chromatographic separation of **CUR** and its derivative was achieved using a Inertsil ODS-SP C18 (5 μm, 4.6 × 150 mm, Shimadzu, Tokyo) column at 30 °C. The injection volume was 10 μL. The mobile phase consisted of 0.1% formic acid in ultra-pure water - methanol (20:80, v/v) at a flow rate of 1 mL/min. The method gave baseline separation of the analytes within a run time of 10 min, and reproducible peak shapes and retention times.

4.4.2. Sample preparation

Excess amounts (~5 mg) of samples were suspended 1 mL ammonia water in 1.5 mL centrifuge tube. These vials were kept in a thermostated oscillator (SHZ-C, Shanghai Boxun Industrial Co., Ltd., China) maintained at 37 °C. After 1 h, the samples were centrifuged at 13000 rpm for 10 min with a microcentrifuge (MicroCL 21, Thermo Scientific Co., USA), and the supernatant was filtered through a 0.22 μm organic membrane and detected by UPLC (Acquity UPLC, Waters Co., USA). All experiments were performed in triplicate.

4.5. Antitumor activity evaluation

4.5.1. Cell culture

The human Hepatocellular carcinoma (HCC) line, HepG2 and SMMC-7721 were cultured in RPMI-1640 medium (Gibco, New York, USA) supplemented with 10% fetal bovine serum (FBS, ScienCell, Carlsbad, CA, USA), 100 U/mL penicillin, 100 μg/mL streptomycin; grown in an atmosphere of 5% CO_2 and 90% humidity at 37 °C. The medium was replaced every 2–3 days after incubation.

4.5.2. Antitumor assays

The half maximal inhibitory concentrations (IC_{50}) of HepG2 and SMMC-7721 cells were determined by the MTT assay. Briefly, cells in logarithmic growth were seeded at 1×10^5 cells/ml and were treated with **CUR** and derivatives **5(a-j)** at various concentrations for 3 days. After 72 h of incubation, 20 μL of 5 mg/mL MTT solution was added to each well and the cells were further incubated for 4 h at 37 °C. Then, the media were removed and 150 μL DMSO was added to each well. The optical density (OD) of each well was measured using a microplate reader at 570 nm (Spark 10M, Tecan, Switzerland). The IC_{50} values of 11 compounds against SMMC-7721 and HepG2 were calculated by GraphPad Prism 7.0 statistical software.

4.6. Uptake and PepT1-mediated experiments

4.6.1. Caco-2 cells culture

Caco-2 cells were cultured in DMEM medium with 10% FBS, 100 U/mL penicillin, 100 μg/mL streptomycin, 1% non-essential amino acid. Culture medium was changed every other day, when the cells reached confluence, they were plated on 24-well dishes at a density of 5×10^4 cells/well. The cell monolayers were given fresh medium every other day and were used on the 15th day for uptake experiments.

4.6.2. LC-MS/MS condition

A Nexera UHPLC 30A LC system (Shimadzu Corporation, Kyoto, Japan) coupled with a QTRAP ™4500 MS system (AB Sciex Corporation., Foster City, CA) was used. Chromatographic separation of **CUR**, **5d**, **5e** and internal standard (Honokiol) was achieved using a Inertsil ODS-SP C18 (5 μm, 4.6 × 150 mm, Shimadzu, Tokyo) column at 40 °C. The injection volume was 2 μL. The mobile phase consisted of 0.1% formic acid in ultra-pure water - methanol (22:78, v/v) at a flow rate of 1 mL/min. Mass spectrometric condition: ionization was achieved using electrospray ionization (ESI) with multi-ion monitoring (MRM) in the negative mode. The optimized quantitative analysis of ion pairs and parameters were described in Table S3 (shown in Supplementary material).

4.6.3. Selectivity

The LC-MS/MS method has high selectivity because only ions derived from the analytes of interest were monitored. The typical MRM chromatograms of a blank cell lysate were shown in Fig. S21 (shown in Supplementary material). No interfering peak was observed in blank cell lysates.

4.6.4. Cell lysate sample preparation

Aliquots of cell lysate (50 μL) were mixed with 50 μL internal standard solution (Honokiol, 200 ng/mL) and 400 μL methanol and vortex-mixed for 3 min. After centrifugation for 10 min at 12,000 rpm at 4 °C. 2 μL of these samples was injected into the LC-MS/MS system for analysis.

The typical equation of calibration curves and linearity ranges for the three analytes as follows: $y = 0.0818x - 0.513$ ($R^2 = 0.9973$) at 1–500 ng/mL of **CUR**, $y = 0.0036x - 0.0085$ ($R^2 = 0.9984$) at 5–500 ng/mL of compound **5d**, $y = 0.0066x + 0.0466$ ($R^2 = 0.9955$)

at 2–500 ng/mL of compound **5e**.

4.6.5. Uptake and uptake inhibition studies

The Caco-2 cells were cultured for 15 days, the culture medium was removed on the day of experiment, and the Caco-2 cell monolayers were washed twice with HBSS (Hyclone, USA), after washing, the cells were preincubated with HBSS for 30 min at 37 °C. The medium was removed after the preincubation period and uptake was initiated by adding 1 mL of the preincubated drug solution. Caco-2 cells were incubated with the drug solution at the appropriate time. The drug solution was aspirated and the cells were then quickly rinsed three times with ice-cold PBS (pH 7.4, Hyclone, USA) to terminate uptake. Then the cells were lysed with 0.3 mL of RIPA lysate, after the cell lysis was completed, the cell lysate was collected, centrifuged at 4 °C, 12,000 rpm for 20 min and a part of the supernatant was used to determine the cellular protein by BCA Protein Assay Kit, the LC-MS/MS was utilized to detect the drug concentration. All experiments were conducted in three independence tests. For time and pH dependence of uptake experiments, the cell monolayers were incubated treated with the drug solution (pH = 6.0 or 7.4) at different time (0, 15, 30, 60, 90 min). For the effect of concentration to cellular uptake of **CUR**, **5d** and **5e** studies, the Caco-2 cells were incubated with uptake buffer (pH = 6.0) containing drug solution at various concentrations (50, 100, 200, 400, 800 μM) for 60 min. In order to evaluate the *in vitro* PepT1 involved in the uptake of **5d** and **5e,** the uptake inhibition test with Gly-Sar was carried out. The Caco-2 monolayers were incubated with **CUR**, **5d** and **5e** (100 μM) in the absence or in the presence of Gly-sar for 60 min at pH = 6.0. To explore the inhibition rate of gly-sar on compounds **5d** and **5e**, Caco-2 monolayers were incubated with **CUR**, **5d** and **5e** at various concentrations (100, 200, 400, 800 μM) in the presence of Gly-sar for 60 min at pH = 6.0.

4.7. In vitro phase I metabolism assay

4.7.1. Incubations with rat liver microsomes for 5d and 5e metabolism

The rat liver microsomes was thawed carefully on ice before the experiment. **CUR**, **5d** and **5e** (20 μM) was incubated with liver microsomes in 200 μL of phosphate-buffered saline (PBS, 100 mM, pH 7.4), containing magnesium chloride (5 mM). Reactions were initiated by the addition of NADPH (1.3 mM). After 2 h of incubation, the reaction was terminated by the addition of 1 mL of ice-cold methanol. Mixtures were vortexed and centrifuged at 12,000*g* for 10 min at 4 °C to precipitate proteins. Supernatants were transferred to fresh tubes and evaporated to dryness. The residues were dissolved in methanol/water (50:50, v/v) for analysis by UFLC-QTOF/MS. All experiments were performed in duplicate. Control incubations were performed without the cofactor NADPH.

4.7.2. LC-QTOF MS condition

A UFLC 20ADXR LC system in-line (Shimadzu Corporation, Kyoto, Japan) coupled with a hybrid quadrupole time-of fight mass spectrometer QTOF MS (Triple TOF™ 5600 MS system, AB Sciex Corporation., Foster City, CA) was used. Chromatographic separation of **CUR**, **5d** and **5e** and its metabolites was achieved using a Inertsil ODS-SP C18 (5 μm, 4.6 × 150 mm, Shimadzu, Tokyo) column at 40 °C. The injection volume was 2 μL. The mobile phase consisted of 0.1% formic acid in ultrapure water - methanol (22:78, v/v) at a flow rate of 1 mL/min. Mass spectrometric condition: MS and MS/MS data were acquired by Analyst® software using a TripleTOF™ 5600 mass spectrometer with MS scan and information dependent acquisition (IDA) MS/MS scans. Ionization was achieved using electrospray ionization (ESI) in the negative mode from *m/z* 50 to 1200 at a source temperature of 500 °C. Nitrogen gas was used as ion source gases and collision gas. The parameters of MS mass spectrometric analysis were as follows: ion Source Gases 1 and 2 (GS1 and GS2), 50 psi; declustering potential, −60 eV; and collision energy (CE) −5eV.

Acknowledgements

This work was supported by the National Science Foundation of China (No. 81573304), and Research Fund for Jiangsu Graduate Research Innovation Program (KYCX18_1595). Thank you for help in instrumental analysis provided by Center for Instrumental Analysis of Nanjing University of Chinese Medicine.

Appendix A. Supplementary data

Supplementary data to this article can be found online at https://doi.org/10.1016/j.bioorg.2019.103163.

References

[1] H.P. Ammon, M.A. Wahl, Pharmacology of Curcuma longa, Planta Medica 57 (01) (1991) 1–7.
[2] B. Li, Y. Hu, Y. Zhao, et al., Curcumin attenuates titanium particle-induced inflammation by regulating macrophage polarizationin vitro and in vivo, Front. Immunol. 8 (9) (2017) 55–65.
[3] J.X. Wu, L.Y. Zhang, Y.L. Chen, et al., Curcumin pretreatment and post-treatment both improve the antioxidative ability of neurons with oxygen-glucose deprivation, Neural Regener. Res. 10 (3) (2015) 481–489.
[4] M. Salem, S. Rohani, E.R. Gillies, Curcumin, a promising anti-cancer therapeutic: a review of its chemical properties, bioactivity and approaches to cancer cell delivery, RSC Adv. 4 (28) (2014) 64–74.
[5] B.B. Aggarwal, Targeting inflammation-induced obesity and metabolic diseases by Curcumin and other nutraceuticals, Annu. Rev. Nutr. 30 (1) (2010) 173–199.
[6] A.L. Cheng, C.H. Hsu, J.K. Lin, et al., Phase I clinical trial of curcumin, a chemopreventive agent, in patients with high-risk or pre-malignant lesions, Anticancer Res. 21 (4B) (2001) 2895–2900.
[7] H. Hatcher, P. Planapl, J. Cho, F.M. Torti, S.V. Torti, curcumin: from ancient medicine to current clinical trials, Cell. Mol. Life Sci. 65 (2008) 1631–1652.
[8] X. Fan, C. Zhang, D. Liu, et al., The clinical applications of curcumin: current state and the future, Curr. Pharm. Des. 19 (11) (2013) 2011–2031.
[9] S. Darvesh Altaf, B. Aggarwal Bharat, Bishayee Anupam, Curcumin and liver cancer: a review, Curr. Pharm. Biotechnol. 13 (2012) 218–228.
[10] R. Afrin, S. Arumugam, A. Rahman, M.I.I. Wahed, V. Karuppagounder, M. Harima, H. Suzuki, S. Miyashita, K. Suzuki, H. Yoneyama, Curcumin ameliorates liver damage and progression of NASH in NASH-HCC mouse model possibly by modulating HMGB1-NF-κB translocation, Int. Immunopharmacol. 44 (2017) 174–182.
[11] D. Xin-Zheng, Y. Hai-Tao, S. Ling-Fei, et al., Potential therapeutic efficacy of curcumin in liver cancer, Asian Pac. J. Cancer Prev. Apjcp 14 (6) (2013) 3855–3859.
[12] S. Shankar, R.K. Srivastava, Curcumin: Structure, Biology and Clinical Applications. Nutrition, Diet and Cancer, Springer, Dordrecht, 2012, pp. 413–457.
[13] P.R.N. Bhuket, A. El-Magboub, I.S. Haworth, P. Rojsitthisak, Enhancement of curcumin bioavailability via the prodrug approach: challenges and prospects, Eur. J. Drug Metab. Pharmacokinet. 42 (3) (2017) 341–353.
[14] S.B. Wan, H. Yang, Z. Zhou, et al., Evaluation of curcumin acetates and amino acid conjugates as proteasome inhibitors, Int. J. Mol. Med. 26 (4) (2010) 447–455.
[15] F. Cao, J. Jia, Z. Yin, et al., Ethylene glycol-linked amino acid diester prodrugs of oleanolic acid for PepT1-mediated transport: synthesis, intestinal permeability and pharmacokinetics, Mol. Pharm. 9 (8) (2012) 2127–2135.
[16] Y. Gong, X. Wu, T. Wang, et al., Targeting PEPT1: A novel strategy to improve the antitumor efficacy of Doxorubicin in human hepatocellular carcinoma therapy, Oncotarget 8 (25) (2017) 40454–40468.
[17] W. Tao, D. Zhao, M. Sun, et al., Enzymatic activation of double-targeted 5′-O-l-valyl-decitabine prodrug by biphenyl hydrolase-like protein and its molecular design basis, Drug Deliv. Transl. Res. 7 (2) (2017) 304–311.
[18] Y. Zhang, J. Sun, Y. Sun, et al., Prodrug design targeting intestinal PepT1 for improved oral absorption: design and performance, Curr. Drug Metab. 14 (6) (2013) 675–687.
[19] K.H. Gilzad, K. Kaur, F. Jamali, Synthesis and characterization of a new Peptide prodrug of glucosamine with enhanced gut permeability, Plos One 10 (5) (2015) e0126786.
[20] P.D. Bailey, C.A. Boyd, J.R. Bronk, et al., How to make drugs orally active: a substrate template for peptide transporter PepT1, Cheminform 31 (16) (2000) 505–508.
[21] B.S. Anand, S. Katragadda, A.K. Mitra, Pharmacokinetics of novel dipeptide ester prodrugs of acyclovir after oral administration: intestinal absorption and liver metabolism, Pharmacology 311 (2004) 659–667.
[22] B.S. Anand, J. Patel, A.K. Mitra, Interactions of the dipeptide ester prodrugs of acyclovir with the intestinal oligopeptide transporter: competitive inhibition of glycylsarcosine transport in human intestinal cell line-Caco-2, J. Pharmacol. Exp. Ther. 304 (2) (2003) 781–791.
[23] A. Ray, K. Cholkar, R. Earla, A.K. Mitra, Doxorubicin prodrug for cytoplasmic and nuclear delivery in breast cancer cells, Drug Develop. Therap. 7 (1) (2016) 13–19.
[24] L.H. Zhang, L. Zhang, T. Luo, Synthesis and evaluation of a dipeptide drug conjugate library as substrates for PEPT1, ACS Comb. Sci. 14 (2012) 108–114.
[25] L. Fang, M. Wang, S. Gou, et al., Combination of amino acid/dipeptide with nitric oxide donating oleanolic acid derivatives as PepT1 targeting antitumor prodrugs, J.

Med. Chem. 57 (3) (2014) 1116–1120.
[26] C. Santos, J. Morais, L. Gouveia, et al., Dipeptide derivatives of AZT: synthesis, chemical stability, activation in human plasma, hPEPT1 affinity, and antiviral activity, ChemMedChem: Chem. Enabling Drug Discov. 3 (6) (2008) 970–978.
[27] R. Jain, S. Duvvuri, V. Kansara, N.K. Mandava, A.K. Mitra, Intestinal absorption of novel-dipeptide prodrugs of saquinavir in rats, Int. J. Pharm. 336 (2007) 233–240.
[28] A.H. Der-Boghossian, S.R. Saad, C. Perreault, et al., Role of insulin on jejunal PepT1 expression and function regulation in diabetic male and female rats, Can. J. Physiol. Pharmacol. 88 (7) (2010) 753–759.
[29] H.Y. Zhang, C. Sun, M. Adu-Frimpong, et al., Glutathione-sensitive PEGylated curcumin prodrug nanomicelles: Preparation, characterization, cellular uptake and bioavailability evaluation, Int. J. Pharm. 555 (2019) 270–279.
[30] N.K. Paul, M. Jha, K.S. Bhullar, et al., All trans 1-(3-arylacryloyl)-3, 5-bis (pyridin-4-ylmethylene) piperidin-4-ones as curcumin-inspired antineoplastics, Eur. J. Med. Chem. 87 (2014) 461–470.
[31] N. Samaan, Q. Zhong, J. Fernandez, G. Chen, A.M. Hussain, S. Zheng, G. Wang, Q.H. Chen, Design, synthesis, and evaluation of novel heteroaromatic analogs of curcumin as anti-cancer agents, Eur. J. Med. Chem. 75 (2014) 123–131.
[32] S. Wang, X. Peng, L. Cui, et al., Synthesis of water-soluble curcumin derivatives and their inhibition on lysozyme amyloid fibrillation, Spectrochim. Acta Part A: Mol. Biomol. Spectrosc. 190 (2018) 89–95.
[33] A. Simon, D.P. Allais, J.L. Duroux, et al., Inhibitory effect of curcuminoids on MCF-7 cell proliferation and structure–activity relationship, Cancer Lett. 129 (1) (1998) 111–116.
[34] K.I. Priyadarsini, Chemical and structural features influencing the biological activity of curcumin, Curr. Pharm. Des. 19 (11) (2013) 2093–2100.
[35] Q. Shi, C. Shih, H. Lee, Novel anti-prostate cancer curcumin analogues that enhance androgen receptor degradation activity, Anticancer Agents Med. Chem. 8 (2009) 904–912.
[36] T. Higuchi, K.A. Connors, Phase-solubility techniques, Adv. Anal. Chem. Instrum. 4 (1965) 117–212.
[37] C. Jaynthy, Aggregational studies of dipeptide from Clostridium strain MP flavodoxin, Asian J. Pharm. Clin. Res. 7 (3) (2014) 200–202.